Electronic Supplementary Material (ESI) for Physical Chemistry Chemical Physics.

Electronic Supporting Information (ESI)

Inversion probability of three-bladed self-propelled rotors after forced stops of different durations

Satoshi Nakata,[a,*] Takero Matsufuji,[a] Jerzy Gorecki,[b] Hiroyuki Kitahata,[c]

and Hiraku Nishimori[a]

a. Graduate School of Science, Hiroshima University, 1-3-1 Kagamiyama, Higashi-Hiroshima, Hiroshima 739-8526, Japan

b. Institute of Physical Chemistry, Polish Academy of Sciences, Kasprzaka 44/52, 01-224 Warsaw, Poland

c. Department of Physics, Graduate School of Science, Chiba University, 1-33 Inage-ku, Chiba 263-8522, Japan

*To whom correspondence should be addressed. Tel. & fax: +81-824-24-7409

E-mail: nakatas@hiroshima-u.ac.jp

1. Shape of the self-propelled rotors as a function of θ

In the present study, we considered θ as the parameter that controls the shape of the self-propelled rotors, as shown in Figure 1a. Figure S1a shows the definition of the parameters, a, b, c, l_1, l_2, l_3, and l_4. For the investigated rotors, a, b, and c were fixed at 20.0, 23.5, and $10.0 \times \sqrt{3}$ mm, respectively. Figure S1b shows l_1, l_2, l_3, and l_4 which depend on θ. Based on Figure S1b, we examined at θ = 60-120 deg since l_3 was negative at $\theta \leq 50$ deg.

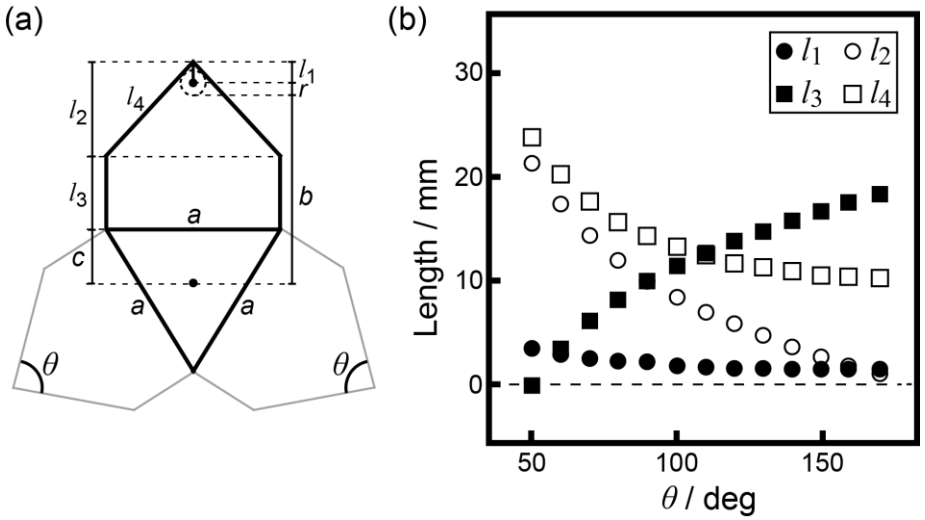

Figure S1. (a) Schematic illustration of the self-propelled rotor and definition of parameters of a, b, c, l_1, l_2, l_3, and l_4, and (b) l_1, l_2, l_3, and l_4 depending on θ. a = 20.0 mm, b = 23.5 mm, $c = \frac{\sqrt{3}}{2}a$, and r = 1.5 mm. $l_1 = \frac{r}{\sin\frac{\theta}{2}}$, $l_2 = \frac{a}{2\tan\frac{\theta}{2}}$, $l_3 = l_1 - l_2 + b + c$, and $l_4 = \frac{a}{2\sin\frac{\theta}{2}}$. The dotted circle in (a) denotes the location of a camphor disk.

2. Movie of the experimental result in Figure 2

Movie S1 corresponds to the self-propelled motion in Figure 2 (4 × speed).

3. Inversion probability for θ = 60, 70, 80, 90, 95, 100, and 120 deg as a function of t_d

Figure S2 shows the experimental results on the inversion probability (*IP*) for the self-propelled rotors shown in Figure 1a, as a function of t_d at different θ (= 60, 70, 80, 90, 95, 100, and 120 deg).

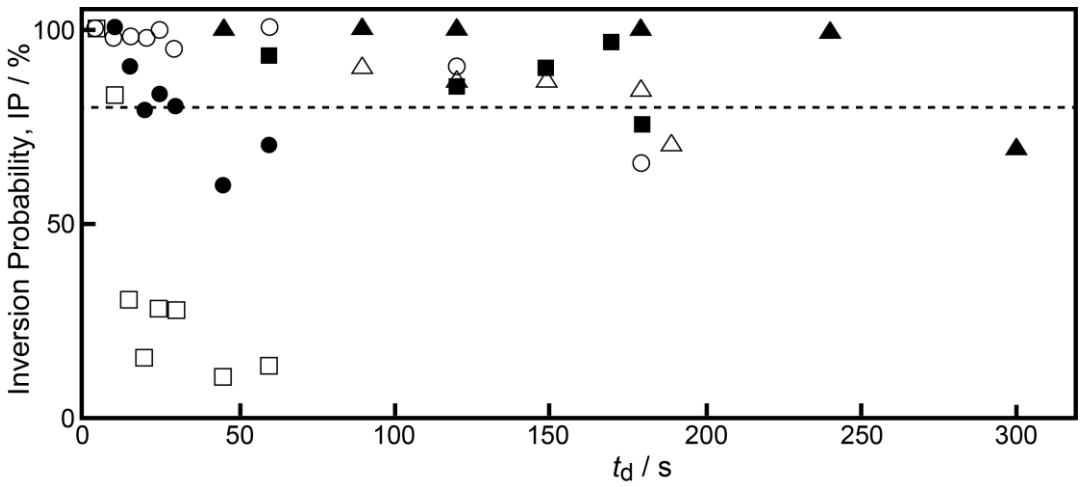

Figure S2. Experimental results on the inversion probability (*IP*) as a function of t_d at different θ (filled triangles: 60 deg, empty triangles: 70 deg, filled squares: 80 deg, empty circles: 90 deg, filled circles: 95 deg, empty squares: 120 deg). Data correspond to those in Figure 3b.

4. Rotation of the self-propelled rotor with three bars to decrease the velocity

To control the angular velocity of the self-propelled rotors with the same shape, three bars (length: l_b) were glued below the three blades, as illustrated in Figure 1b. Figure S3 shows the angular velocity of the self-propelled rotor characterized at θ = 70 deg as a function of l_b. The angular velocity decreased with an increase in l_b.

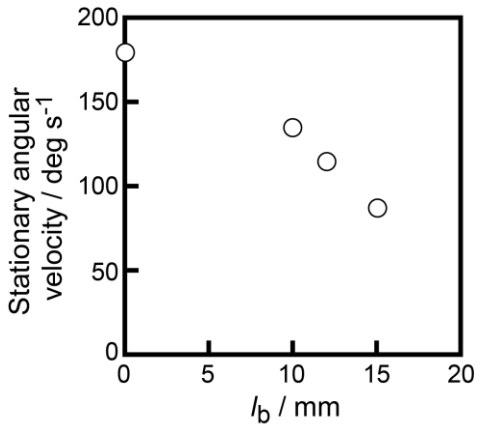

Figure S3. Experimental results on the stationary angular velocity depending on the length of the bars, l_b, for the self-propelled rotor at $\theta = 70$ deg (see Figure 1b).

5. Visualization of the distribution of camphor molecules developed from the rotor

To visualize the camphor molecules developed from camphor disks at the blade corners to the water surface, the water surface was covered with $CaCO_3$ powders (see Figure 6). The contact lengths corresponding to high concentration of camphor molecules (l_{hr} and l_{hl}) were measured for the individual corners at the halting state just before releasing, and averaged as shown in Figure 6a. The difference between l_{hr} and l_{hl} (Δl_h) increased with an increase in the angular velocity, as shown in Figure S4.

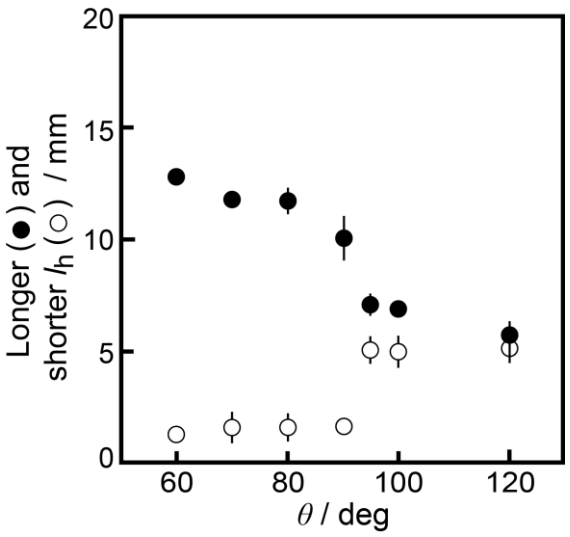

Figure S4. Experimental results on longer (filled circles) and shoter l_h (empty circles) contact lines as functions of the angle, θ. The values of l_h were the averaged over values for three blades.

To calculate the torque of the self-propelled rotor during rotation, l_{rr} and l_{rl} were measured during the rotation, as shown in Figure S5. Actually, l_{rr} and l_{rl} could not be measured at the stationary state since the distribution of camphor was perturbed by the rotation of the blades. Therefore, l_{rr} and l_{rl} in Figure S5 were measured before the rotor reached its stationary angular velocity, and they were used as the values corresponding to the stationary angular velocity in our calculations of the torque. The angular velocity used in Figure S5 was measured with $CaCO_3$ powders added to the water surface when the rotor reached the stationary angular velocity.

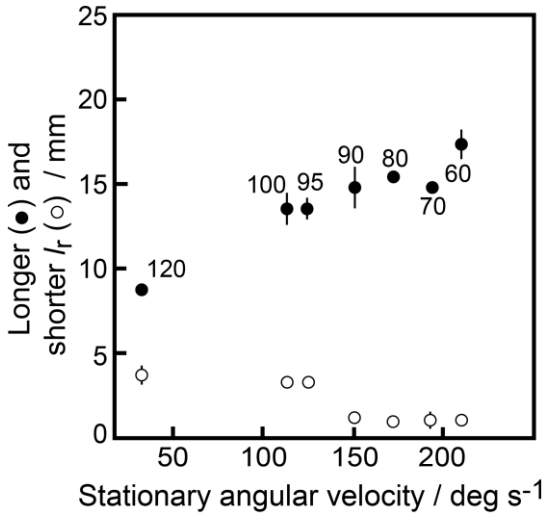

Figure S5. Longer and shorter l_r measured during the rotation as functions of the stationary angular velocity of the rotor. The rotors illustrated in Figure 1a were used in this experiment. The numbers denote the angle, θ, in the unit of degree of the rotor. The plotted values of l_r were averaged over three blades.

5. Calculation of torque of the self-propelled rotor as a function of θ

We calculate the torque working on the self-propelled rotor, $N(\theta)$. Figure S6 shows the schematic illustration on the calculation of $N(\theta)$.

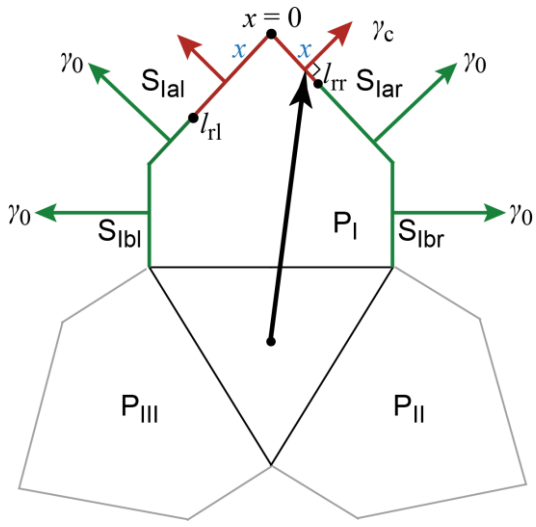

Figure S6. Schematic illustration of the self-propelled rotor to calculate the torque, $N_{\mathrm{Iar}}(\theta)$. $\mathrm{P_I}$, $\mathrm{P_{II}}$, and $\mathrm{P_{III}}$ are three blades. $\mathrm{S_{Ial}}$, $\mathrm{S_{Ibl}}$, $\mathrm{S_{Iar}}$, and $\mathrm{S_{Ibr}}$ are the sides in $\mathrm{P_I}$. γ_c and γ_0 are the surface tension of camphor and pure water ($\gamma_c < \gamma_0$). The green and red parts of the contour denote the regions where the surface tension is γ_0 and γ_c, respectively.

Here, three blades in the rotor are distinguished by $\mathrm{P_I}$, $\mathrm{P_{II}}$, and $\mathrm{P_{III}}$. $\mathrm{S}n\mathrm{a}$ and $\mathrm{S}n\mathrm{b}$ are two sides of $\mathrm{P}n$ (n = I, II, or III) with the length of l_4 and l_3, respectively. $\mathrm{S}n\mathrm{r}$ and $\mathrm{S}n\mathrm{l}$ are the right and left sides of $\mathrm{P}n$ (n = I, II, or III). We assume that the surface tension of pure water, γ_0, works at $\mathrm{S}n\mathrm{b}$ (n = I, II, or III) and that the blades and distributions of surface camphor concentration around them are identical. As the force of $\mathrm{S}n\mathrm{br}$ is balanced at that of $\mathrm{S}n\mathrm{bl}$, we consider the force at $\mathrm{S}n\mathrm{ar}$ and $\mathrm{S}n\mathrm{al}$. $N_{\mathrm{Iar}}(\theta)$ is the torque working on the side S_{Iar}. $N_{\mathrm{Iar}}(\theta)$ at $\mathrm{S_{Iar}}$ is obtained as.

$$N_{\mathrm{Iar}}(\theta) = \int_0^{l_{\mathrm{rr}}} \gamma_{\mathrm{c}} \left[(b + l_1)\cos\frac{\theta}{2} - x\right] dx + \int_{l_{\mathrm{rr}}}^{l_4} \gamma_0 \left[(b + l_1)\cos\frac{\theta}{2} - x\right] dx$$

$$= \gamma_{\mathrm{c}} \left[l_{\mathrm{rr}}(b + l_1)\cos\frac{\theta}{2} - \frac{l_{\mathrm{rr}}^2}{2}\right] + \gamma_0 \left[(l_4 - l_{\mathrm{rr}})(b + l_1)\cos\frac{\theta}{2} - \left(\frac{l_4^2 - l_{\mathrm{rr}}^2}{2}\right)\right], \qquad \text{(S1)}$$

where x is the coordinate along $\mathrm{S_{Iar}}$ from the edge of $\mathrm{P_I}$ (x = 0) and l_{r} is the contact length from x = 0. We assume that the surface tension at $0 \le x \le l_{\mathrm{r}}$ is γ_c when camphor molecules are developed from $\mathrm{S_{Iar}}$ to the water surface and that the surface tension at $x > l_{\mathrm{r}}$ is γ_0 during the release operation.

On the other hand, $N_{\mathrm{Ial}}(\theta)$ at $\mathrm{S_{Ial}}$ is obtained as.

$$N_{\mathrm{Ial}}(\theta) = -\gamma_{\mathrm{c}} \left[l_{\mathrm{rl}}(b + l_1)\cos\frac{\theta}{2} - \frac{l_{\mathrm{rl}}^2}{2}\right] - \gamma_0 \left[(l_4 - l_{\mathrm{rl}})(b + l_1)\cos\frac{\theta}{2} - \left(\frac{l_4^2 - l_{\mathrm{rl}}^2}{2}\right)\right]. \qquad \text{(S2)}$$

Here, we assume that the surface tension is γ_0, i.e., there is no development of camphor molecules from $\mathrm{S_{Ial}}$ during the release operation. Finally, the torque of the rotor, $N(\theta)$, is described as follows, which corresponds to eq 1 in the main text.

$$N(\theta) = N_{\mathrm{Iar}} + N_{\mathrm{IIar}} + N_{\mathrm{IIIar}} + N_{\mathrm{Ial}} + N_{\mathrm{IIal}} + N_{\mathrm{IIIal}} = 3(N_{\mathrm{Iar}} + N_{\mathrm{Ial}})$$

$$= 3(\gamma_{\mathrm{c}} - \gamma_0)\left[\frac{l_{rl}^2 - l_{rr}^2}{2} - (l_{rl} - l_{rr})b\cos\theta + r\cot\theta\right]. \quad (1)$$

6. Estimation of the Marangoni number and the Peclet number in the present system

We can estimate the Marangoni number and the Peclet number. Here, "solutal" Marangoni number is important and it is defined as $(\partial\gamma/\partial c)(\Delta cL/\eta D) = \Delta\gamma L/\eta D$, where $\Delta\gamma$ is the difference by the camphor dissolution, L is the typical length of the blade, η is the viscosity of water, and D is the diffusion coefficient. When $\Delta\gamma \sim 0.01$ N m^{-1}, $L \sim$ 0.01 m, $\eta \sim 10^{-3}$ Pa s, and $D \sim 10^{-9}$ m^2 s^{-1}, $Ma \sim 10^8$, which means strong Marangoni flow occurs. As for the Peclet number, it is defined as $Pe = L\upsilon/D$, where υ is the typical velocity. Here, $\upsilon \sim 0.01$ m s^{-1}, and thus $Pe \sim 10^5$. This means the advective transport is more important than the diffusive transport for this system.